Journal of Traditional and Complementary Medicine xxx (xxxx) xxx

Contents lists available at ScienceDirect

Journal of Traditional and Complementary Medicine

journal homepage: www.elsevier.com/locate/jtcme

Spatholobus suberectus Dunn inhibits breast cancer bone metastasis *in vitro* and *in vivo*

Qingqing Liu [a,b,1], Nanxi Li [c,1], Dijie Li [d], Feng Zhang [a,b], Yang Jiang [e], Kumar Ganesan [a,b], Yue Sui [a,b], Jin Liu [c,**], Jianping Chen [a,b,*]

[a] School of Chinese Medicine, Li Ka Shing Faculty of Medicine, The University of Hong Kong, China
[b] Shenzhen Institute of Research and Innovation, The University of Hong Kong, Shenzhen, Guangdong, China
[c] Law Sau Fai Institute for Advancing Translational Medicine in Bone and Joint Diseases (TMBJ), School of Chinese Medicine, Hong Kong Baptist University (HKBU), China
[d] Guangxi Universities Key Laboratory of Stem Cell and Biopharmaceutical Technology, College of Life Sciences, Guangxi Normal University, Nanning, Guangxi Province, China
[e] The Department of Traditional Chinese Medicine, Beijing Jishuitan Hospital, Beijing, China

ARTICLE INFO

Keywords:
Spatholobus suberectus
Breast cancer
Bone metastasis
Osteoclasts differentiation
RAW264.7

ABSTRACT

Background and aim: Breast cancer bone metastasis (BCBM) has a high incidence in clinical settings, resulting in decreased life expectancy and quality of life. Previous research has shown that *Spatholobus suberectus* Dunn inhibits breast cancer lung metastasis. However, no studies have examined its regulatory effects on BCBM. Hence, the present study aimed to investigate the inhibitory effect of the percolation of *Spatholobus suberectus* (SSP) on BCBM and its underlying mechanisms.

Experimental procedure: The inhibitory role of SSP on BCBM was determined by cytotoxicity, colony formation assays, invasion, and migration in triple-negative breast cancer (TNBC) cells, and osteoclast differentiation in RANKL-induced RAW 264.7 cell lines. The progression of bone metastasis and overall survival of mice were determined using the BCBM mouse model.

Results and conclusion: SSP treatment significantly reduced TNBC proliferation, migration, invasion, and colony formation and inhibited osteoclast differentiation. Additionally, SSP significantly decreased the expression of bone-related marker genes, such as tartrate-resistant acid phosphatase, cathepsin K, and osteoclast-associated receptors. SSP administration effectively reduced the progression of bone metastasis and prolonged the survival time of mice compared to that of the control. The expression level of Dickkopf-1 was also downregulated after SSP treatment, which may account for SSP's anti-bone metastasis mechanism. Overall, SSP exerts therapeutic effects by mitigating colony formation, invasion, migration, metastasis, osteoclast differentiation, and osteolytic destruction. This may provide new drugs for the prevention and treatment of BCBM.

1. Introduction

Breast cancer (BC) is the most common female malignancy, and its morbidity ranks first among tumor diseases in the world.[1] Breast (73 %) and prostate cancers (68 %) have the highest prevalence in terms of the incidence of distant bone metastasis.[2,3] Bone metastasis of tumors is usually divided into three different types: osteolytic type, osteogenic type, and mixed type. It is believed that breast cancer bone metastasis (BCBM) primarily manifests as osteolytic injury.[4] As a result of the structural damage to the bone tissue caused by metastasis, individuals with bone metastases frequently experience symptoms like bone pain, osteoporosis, nerve compression, and hypercalcemia, collectively referred to as skeletal-related events (SREs). SRE are typically correlated with impaired mobility and reduced social functioning, leading to a decline in quality of life, poorer survival rates, and increased healthcare expenditures. are often linked to a decline in mobility and social interaction, resulting in a lower quality of life, reduced survival rates, and higher healthcare expenses.[5] Severe bone pain is the most prevalent

* Corresponding author. School of Chinese Medicine, Li Ka Shing Faculty of Medicine, The University of Hong Kong, China.
** Corresponding author.
E-mail addresses: liujin@hkbu.edu.hk (J. Liu), abchen@hku.hk (J. Chen).
[1] These authors have contributed equally to this work.

https://doi.org/10.1016/j.jtcme.2024.11.013
Received 8 May 2023; Received in revised form 30 August 2024; Accepted 21 November 2024
Available online 24 November 2024

SRE, affecting around 80 % of individuals with bone metastases.[6] Detecting bone metastases at an earlier stage of the disease could enable proactive interventions, potentially reducing the occurrence of SREs, maintaining functionality, and preserving quality of life.[7] Therefore, the prevention and treatment of BCBM are of great significance to clinical management.

Generally, bone formation and resorption occur continuously in bone tissue, resulting in osteoblasts and osteoclasts, called bone remodeling.[8] The secondary damage of osteolytic bone lesions is mainly caused by metastatic tumor cells breaking the original bone homeostasis. This overstimulates osteoclasts maturation and inhibits bone formation, resulting in bone loss and osteolysis.[4] The vicious cycle initiated by BC cells was widely accepted to explain osteolytic bone metastases. Briefly, metastatic BC cells produce a variety of proteins and cytokines, such as parathyroid hormone-related peptide (PTHrP) to stimulate osteoblasts to express receptor activator of nuclear factor kappa B ligand (RANKL). Next, RANKL can combine with RANK receptor of pre-osteoclasts to promote the growth and differentiation of pre-osteoclasts, resulting in more activated osteoclasts. Bone destruction continues when mature multi-nucleated osteoclasts secrete acids and enzymes such as metalloproteinases (MMPs). Then, bone matrix absorption releases Ca^{2+} and various growth factors into the bone microenvironment, such as transforming growth factor-β (TGF-β). Following this, the release of related growth factors can promote the survival and proliferation of cancer cells, leading to aggravated osteolytic bone damage and tumor progression.[4,7,9] In order to interrupt this vicious cycle, a multi-pronged approach such as targeting cancer cell proliferation, cytokine secretion, osteoclast differentiation process and activation to obtain and provide a favorable systemic microenvironment would be effective.

Traditional Chinese medicine (TCM) has unique advantages in managing human body condition with safety and effectiveness. The *Spatholobus suberect* Dunn (SS, also known as Ji Xue Teng) has been used in China since *Qing* dynasty. In the Chinese Pharmacopoeia, SS was used to treat anemia, irregular menstruation, and rheumatic arthralgia.[10] Modern pharmacological experiments have proved that SS has significant anti-cancer activity against various tumors.[11–20] Evidence suggests that SS exhibits beneficial effects in treating leiomyoma, breast cancer, glioblastoma, and leukemia.[11,12] Among these, the anti-breast cancer properties of SS have garnered significant research interest. SS shows promising anticancer effects by inducing apoptosis and pyroptosis, arresting cell cycle progression, reducing estrogen receptor activity, inhibiting proteasomes, preventing mutations, and regulating reactive oxygen species.[11,15,18,20,21] KEGG and GO analysis indicated that SS may mitigate lung metastasis primarily by modulating oxidative stress, AGE-RAGE signaling, and microRNAs.[22] Additionally, network pharmacology analysis demonstrated that SS could effectively combat ovarian cancer by activating key proteins such as GSK-3β, Bcl-2, and Bax.[23] SS exert their anti-tumor effects by modulating the PI3K/Akt/mTOR and Ras/Raf/MAPK pathways, thereby preventing the development of BC.[21] SS contains a variety of distinguished polyphenolic compounds, such as flavonoids, chalcone, dihydroflavone, pterocarpan, and phenolic acid. These compounds exhibit a range of pharmacological effects, including antioxidant, antidiabetic, antimicrobial, hematological, neuroprotective, and anticancer properties.[12,21]

SS was also reported to have effects on the stromal cells of bone microenvironment. SS could inhibit RANKL-induced osteoclast differentiation,[24,25] *Porphyromonas gingivalis*-induced bone loss,[26] and promote chondrogenesis[25] to apply in bone-related diseases such as osteoarthritis, osteoporosis and periodontitis. These results suggest that SS probably has inhibitory effects on tumor-induced bone resorption, particularly osteolytic bone metastasis. However, there is still a lack of studies on the regulatory effect of SS on the process of breast cancer induced-bone metastasis, especially *in vivo* models. Therefore, in the present study, we aimed to explore the anti-breast cancer bone metastasis effects of SSP (percolated extract of SS in ethanol) and its mechanism. A triple-negative breast cancer (TNBC) cell line, MDA-MB-231, was prepared using the conditioned medium for simulating the pathological state of BC, and murine osteoclast precursor cell, RAW264.7, was used to investigate the effect of SSP on cell proliferation, and the ability of osteoclasts differentiation induced by RANKL. A *in vivo* bone metastasis model was also built to determine the inhibitory efficacy of SSP on BCBM.

2. Materials and methods

2.1. Percolation extract of Spatholobus suberectus Dunn by ethanol (SSP)

The herbal extract has been described above and previously published.[12] Briefly, SSP was extracted from Spatholobus suberectus Dunn (Guangxi Province, Southern China) by percolation with ethanol and water (60:40). The extracted solution was concentrated by rotary evaporation, and the product was then collected by freeze-drying with a vacuum freeze dryer. SSP powder was dissolved in DMSO and then diluted with cell culture medium for further experimentation (the final concentration of DMSO was less than 0.1 %).

2.2. Cell culture

For BC cell lines, MDA-MB-231 and luciferase-labeled MDA-MB-231 cells (MDA-MB-231-Luc) were cultured in DMEM with 10 % fetal bovine serum (FBS) and 1 % penicillin and streptomycin (P/S). BT-549 cells were cultured in RPMI 1640 medium with 10 % FBS and 1 % P/S. For pre-osteoblasts, the MC3T3-E1 cell line was maintained in α-MEM, supplemented with 10 % FBS and 1 % P/S. For, pre-osteoclasts, the RAW264.7 cell line was maintained in DMEM with 10 % FBS, and 1 % P/S. Cell culture medium was replaced every 1–3 days, and cells were passaged using standard cell culture techniques at 70%–90 % confluence. Luciferase-tagged MDA-MB-231 cells were created using lentiviral vectors containing the luciferase reporter gene and all other cell lines were obtained from ATCC; low-passage cells were used for experiments. Cell culture reagents were purchased from Gibco, Thermo Fisher. All cells were maintained in a humidified incubator at 37 °C with 5 % CO_2.

2.3. Breast cancer bone metastasis model in vivo

Bone metastasis experiments were conducted on female BALB/cAnU-nu nude mice, as described previously.[27] MDA-MB-231-Luc cells were harvested and suspended in PBS at a density of 5×10^6 cells per ml, and then they were injected into the left cardiac ventricle in a total volume of 100 μL per mouse. On the following day, mice were randomly grouped by their body weight into two groups: vehicle control group and SSP treatment group (n = 8 per group). The SSP treatment group was administrated orally once per day at 0.4 g/kg/day. Monitoring for mice situations occurred daily, and bone metastases situations were monitored weekly by using the PE IVIS Spectrum *in vivo* imaging system after intraperitoneal injection of D-luciferin at 150 mg/kg (Gold Biotechnology, USA). All animal studies were performed according to ethics recommendations and animal welfare standards and all experimental procedures were approved by the licensing Committee on the Use of Live Animals in Teaching and Research (CULATR No. 5161-19) of the University of Hong Kong.

2.4. MTT and MTS assay

For inhibitory effects of SSP on cancer cell growth experiments, cell viability was initially performed with an MTS Kit (Promega, USA). Cells (MDA-MB-231 and BT-549) were seeded into 96-well microculture plates at 2000 cells per well and allowed to attach for 24 h, then treated with different concentrations of SSP for 24 h, 48 h, and 72 h. Following drug treatment, MTS was incubated for 2–4 h, and absorbance at 490 nm was quantified using a microplate reader. Cell viability in each group was calculated by normalizing the absorbance value to the value of

control cells.

For SSP's effects on RAW 264.7 and MC3T3-E1 cells, cell viability was estimated by the 3-(4,5-dimethylthiazol-2-yl)-2,5-diphenyltetrazolium bromide (MTT) assay, which was performed according to the manufacturer's protocol. The cells were planted in 96-well plates at a density of 1.5×10^4 cells per well. After overnight attachment, different concentrations of SSP extract were placed into each group. After another 24 h of treatment, add MTT solution (Sigma, USA) to each well, and incubate the plate at 37 °C for 4 h. Then, remove the supernatant solution and add 150 μL DMSO to each well. Place the plate on a shaker at low speed for 10 min to fully dissolve the crystals. The optical density (OD) of each well was determined at 490 nm using a microplate reader.

For the influence of MDA-MB-231 conditioned medium on RAW 264.7 proliferation, cell viability was tested by the MTT assay. RAW 264.7 cells were seeded into 96-well plate. For the next 24 h, the culture medium was replaced with a fresh medium containing different percentages of MDA-MB-231 conditioned medium. At the end of the incubation, MTT reagent was added and detected as described above.

2.5. Colony formation assay

The growth potential of BC cells was determined by a colony formation assay. Briefly, 500 cells per well of a six-well plate were seeded and then treated with vehicle control or drugs on the next day, and the culture medium was refreshed every 3 days for 10–15 days in total. At the endpoints of colony formation assays, cells were fixed with 4 % paraformaldehyde (PFA), stained with crystal violet (Sigma, USA), and photographed.

2.6. Wound healing assay

The effect of SSP on cell migration was assayed by a wound-healing assay. Briefly, cells were cultured to confluence in 12-well plates. A wound was created by scraping the cells using a 200 μL pipette tip, and after washing with PBS to remove cellular debris, the medium was replaced with fresh medium with or without drugs. Images were captured immediately after the scratch (0 h), 24 h later, and 48 h later. Cell migration rate was quantified by the area of the gap using ImageJ software. The data were normalized to the average area of the wound at time 0.

2.7. Transwell assay

Transwell chambers (Corning, #3422, USA) were used for invasion assays. First, diluted Matrigel (BD Biosciences, USA) was pre-coated on the top side of the insert membrane and kept in the incubator for 1–2 h. Then 2×10^4 cells in 100 μL serum-free medium were added to the upper chamber, while 500 μL of medium with 10 % FBS was added to the lower chamber. After overnight, another 100 μL serum-free medium with or without drugs was added on the top side, and the chambers were incubated for another 48 h. The noninvasive cells on the top side of the insert membrane were gently removed by scrubbing with cotton swabs. Cells adhering to the bottom of the membrane were fixed in 4 % PFA, stained with crystal violet, and photographed under a microscope (Olympus BX43, Japan). Finally, the number of invasive cells was counted in five randomly selected fields.

2.8. Preparation of conditioned medium (CM)

The MDA-MB-231 cells were plated in T_{25} culture flasks at a density of 1×10^6 cells and incubated at 37 °C. When the cells were at 70 %–80 % confluence, the medium was changed to serum-free DMEM with or without SSP supplement. After incubating for another 24 h, conditioned medium (CM) can be obtained by collecting the medium and centrifuging at 2000×*g* for 10 min to remove cell debris. The CM was frozen at −80 °C for long-term preservation. To conduct further experiments, add different percentages of fresh medium containing 10 % FBS.

2.9. TRAP staining assay

The ability of SSP to influence osteoclast differentiation from pre-osteoclasts was examined. Here murine RAW264.7 cells were used as osteoclast precursor cells, and TRAP-positive cells with three or more nuclei were counted as mature osteoclasts. Following, the RAW264.7 cells were planted in 12-well plates at a density of 6×10^4 cells per well. After cell attachment, replace the old medium with fresh medium supplemented with RANKL (final concentration: 10 ng/mL), with the CM of MDA-MB-231 cells, with or without different concentrations of SSP for osteoclast culture. The culture media were replaced every two days and $TRAP^+$ multinuclear cells were detected using a TRAP staining kit (Sigma, USA) after being incubated for seven days. Cells were then fixed with 4 % PFA for 10 min at room temperature, stained with a TRAP staining kit, and observed under the microscope to capture 5–10 pictures of each well and count the number of mature osteoclasts (≥3 nuclei).

2.10. Real-time quantitative PCR

The mRNA expression level of related genes was measured by a real-time quantitative PCR assay. Total RNAs from RAW264.7 and MDA-MB-231 cells with different treatments based on the experiment design were collected and extracted with the TRIzol reagent (Thermo Fisher, USA). Then, the RNAs were reverse transcribed into cDNA with the High-Capacity RNA-to-cDNA Kit (Thermo Fisher, USA), and frozen at −80 °C for long-term preservation. According to the manufacturer's instructions, fluorescence real-time quantitative PCR was carried out in a reaction mixture that contained 10 μL SYBR® Select Master Mix (Thermo Fisher, USA), 1 μL upper and lower primers, 2 μg cDNA, and 7 μL distilled water. A $2^{-\Delta\Delta Ct}$ method was performed for data analysis, and relative quantification was determined by normalization to the internal reference β-actin. The mRNA expression level of OSCAR was detected by using the TaqMan method (TaqMan Universal Master Mix II with UNG, ThermoFisher, USA, Cat. No: 4440044). The primer sequences are listed in Table 1.

2.11. Western blotting

Standard western blotting was conducted as follows. After treatment, cells were washed with cold PBS twice and harvested by scrapers with radioimmunoprecipitation assay lysis buffer (RIPA, Sigma, USA) supplemented with a protease inhibitor cocktail (Thermo Scientific, USA). After collecting the protein supernatant, the amount was quantitated using the BCA protein assay kit (Thermo Scientific, USA), as the manufacturers' manuals indicated, and then was recovered for sodium dodecyl sulfate-polyacrylamide gel electrophoresis (SDS-PAGE) to separate the proteins. Next, the proteins were transferred to polyvinylidene difluoride (PVDF) membranes (Millipore, USA) for further analysis. Following, membranes were blocked with 3–5% bovine serum albumin (BSA, Sigma, USA) in 1 × TBS-T buffer at room temperature for

Table 1
Primer sequences of osteoclast markers for RT-PCR analysis.

Genes	Primer sequences
TRAP	F: 5′-GCCAAGATGGATTCATGGGTGG-3′ R: 5′-CAGAGACATGATGAAGTCAGCG-3′
CTSK	F: 5′-GATGCTTACCCATATGTGGGC-3′ R: 5′-CATATCCTTTGTTTCCCCAGC-3′
DKK1	F: 5′-ATAGCACCTTGGATGGGTATTCC-3′ R: 5′-CTGATGACCGGAGACAAACAG-3′
β-actin	F: 5′-TCCTGTGGCATCCACGAAACT-3′ R: 5′-GAAGCATTTGCGGTGGACGAT-3′
OSCAR	Mm01338227_g1
β-actin	Mm02619580_g1

1 h and were incubated with the primary antibodies (anti-CXCR4, abcam #ab124824; anti-Vimentin, CST #5741; anti-GAPDH, Immunoway, YM3029; anti-CTSK, abcam #ab19027; anti-α-Tubulin, Sigma, T6793) at 4 °C for overnight. After washing three times in TBS-T for 15 min each, PVDF membranes were probed with horseradish peroxidase (HRP)- conjugated secondary antibodies at room temperature for 1–2 h. After another five times of washing with 1 × TBST buffer, protein bands were visualized by an enhanced chemiluminescent reagent (Millipore, USA).

2.12. Statistical analysis

The statistical analysis was performed with GraphPad Prism 9.0 software. Data were presented as mean ± standard deviation (SD), and results with P values ≤ 0.05 were considered statistically significant. Compared with the control group, *P < 0.05, **P < 0.01 and ***P < 0.001 were presented as indicated.

3. Results

3.1. SSP attenuates the proliferation, migration, invasion, and colony formation of TNBC cell lines

The proliferation, colonization and metastasis of tumor cells are key research directions for the discovery of anti-cancer drugs. To determine the direct regulatory effects of SSP on BC, TNBC cell lines, MDA-MB-231 and BT-549, were used to investigate their proliferation, colony formation, migration, and invasion abilities. The results showed that SSP inhibited MDA-MB-231 and BT-549 cell viability in a dose- and time-dependent manner at 150 μg/mL (Fig. 1a). Next, in Fig. 1b, SSP significantly suppressed the colony formation of both cell lines. The migration ability of BC cells was measured by a wound healing assay, and the

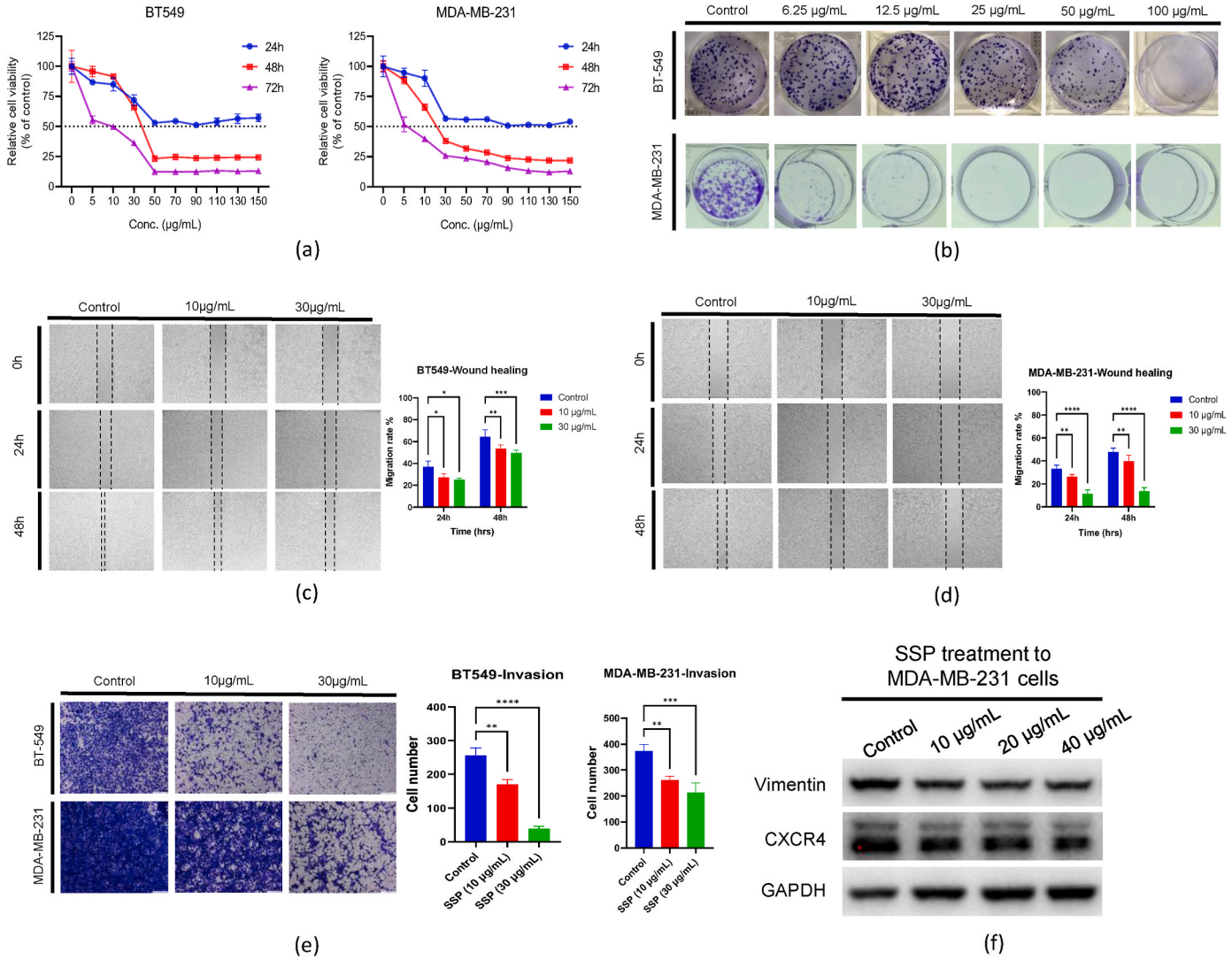

Fig. 1. SSP attenuates the proliferation, migration, invasion, and colony formation of breast cancer cells MDA-MB-231 and BT-549. (a) Cell viability of BT-549 and MDA-MB-231 cells after SSP treatment for 24 h, 48 h, and 72 h was measured by MTS assay. (b) The colony formation ability of BT-549 and MDA-MB-231 cells after SSP treatment (ranging from 6.25 μg/mL to 100 μg/mL) was measured by a colony formation assay. Wound-healing assays of BT-549 (c) and MDA-MB-231 (d) cells after SSP treatment (dose: 10 μg/mL, 30 μg/mL) were used to evaluate migration ability. The representative result shown here was captured under 4 × objective magnification, and the quantitative analysis of migrated area percentage was determined by Image J software. (e) A matrigel-coated transwell assay of MDA-MB-231 and BT-549 cells after SSP treatment (dose: 10 μg/mL, 30 μg/mL) was used to measure invasion ability. The representative result shown here was captured under 10 × objective magnification, and the quantitative analysis of invasive cells was performed in pictures of five random fields under 20 × objective magnification. (f) The expression levels of vimentin and CXCR4 were determined by a western blotting assay after SSP treatment in MDA-MB-231 cells. The experiments were performed at least three times; values are presented as the mean ± SD and representative pictures are illustrated. Data were analyzed in GraphPad Prism 9.0. *P < 0.05, **P < 0.01 and ***P < 0.001 as compared with the control.

matrigel-coated transwell assay that mimicked tumor cells' invasion process. Data in Fig. 1c–e indicated that at doses of 10 and 30 μg/mL of SSP treatment, the number of invasive cells was reduced and the confluence of wound healing also significantly slowed down, indicating that SSP had anti-migration and invasion ability. In the epithelial–mesenchymal transition (EMT) process, vimentin is one of the mesenchymal markers and promotes the tumor invasive phenotype.[28] The C-X-C motif chemokine receptor 4 (CXCR4) of BC cells is more likely to travel to other organs, including bone marrow, where they express its ligand C-X-C motif chemokine ligand 12 (CXCL12), which induces downstream signaling pathways,[7,29] In Fig. 1f, the protein expression levels of both vimentin and CXCR4 were decreased after SSP treatment for 24 h. Based on these findings, we confirmed that SSP may inhibit BC induced bone metastasis.

3.2. SSP restrains RANKL-induced osteoclastic differentiation in RAW 264.7 cells

Before the osteoclastic differentiation assays, MTT assay was used to evaluate the cytotoxicity of different concentrations of SSP (6.25–800 μg/mL) on the mouse-derived osteoclast precursor cell (RAW 264.7) and pre-osteoblasts (MC3T3-E1). As shown in Fig. 2a, the IC_{50} value of SSP extract in RAW264.7 was 154.8 μg/mL, so we kept 6.25–100 μg/mL as the safe concentration range of SSP extract in RAW264.7. Similarly, the IC_{50} value of SSP extract in MC3T3-E1 was 444.4 μg/mL, and SSP extract showed a stimulatory effect on the proliferation of pre-osteoblasts at a concentration of 6.25–200 μg/mL (Fig. 2b). These data revealed that SSP, at least within a concentration of 100 μg/mL, had a significant inhibitory effect on BC cells but showed negligible cytotoxicity to pre-osteoclasts (RAW 264.7) and pre-osteoblasts (MC3T3-E1).

RAW264.7 cells can differentiate into functional osteoclasts under the induction of RANKL, which is a classical method for studying osteoclast differentiation *in vitro*.[30] To observe the effects of SSP on osteoclast differentiation, RAW 264.7 cells were treated with RANKL (10 ng/mL) and different concentrations of SSP (50, 75, 100, 150 μg/mL) for 7 days. At the endpoint, mature osteoclasts were formed, which were detected by tartrate-resistant acid phosphatase (TRAP) staining. As shown in Fig. 2c and d, SSP treatment significantly reduced the number of multinuclear osteoclasts when compared to a control group that treated with only RANKL. This data suggests that SSP restrains RANKL-induced differentiation of pre-osteoclasts (RAW264.7).

TRAP is highly expressed in mature osteoclasts and serves as a specific marker that can reflect the maturity and function of osteoclasts.[31,32] Cathepsin K (CTSK), one of the proteolytic enzymes, plays a crucial role in dissolving the bone matrix after mature osteoclasts attach to bone.[33] The efficacy of several CTSK inhibitors (CKIs) on bone metastasis have already been investigated in clinical trials.[34] The osteoclast-associated receptor (OSCAR) is widely accepted to regulate osteoclastic differentiation, and OSCAR-positive cells can be purified as mature osteoclasts.[27,30,35] The anti-osteoclastogenesis effects of SSP were further proved by assessing the gene expression level of these osteoclast-specific markers by qPCR assay. SSP treatment significantly repressed the mRNA expression of osteoclast-specific marker genes (*Trap, Ctsk,* and *Oscar*) compared to the control group (Fig. 2e). Collectively, these results indicated that SSP interfered with RANKL-induced osteoclast maturation and gene expression of related markers in RAW 264.7 cells.

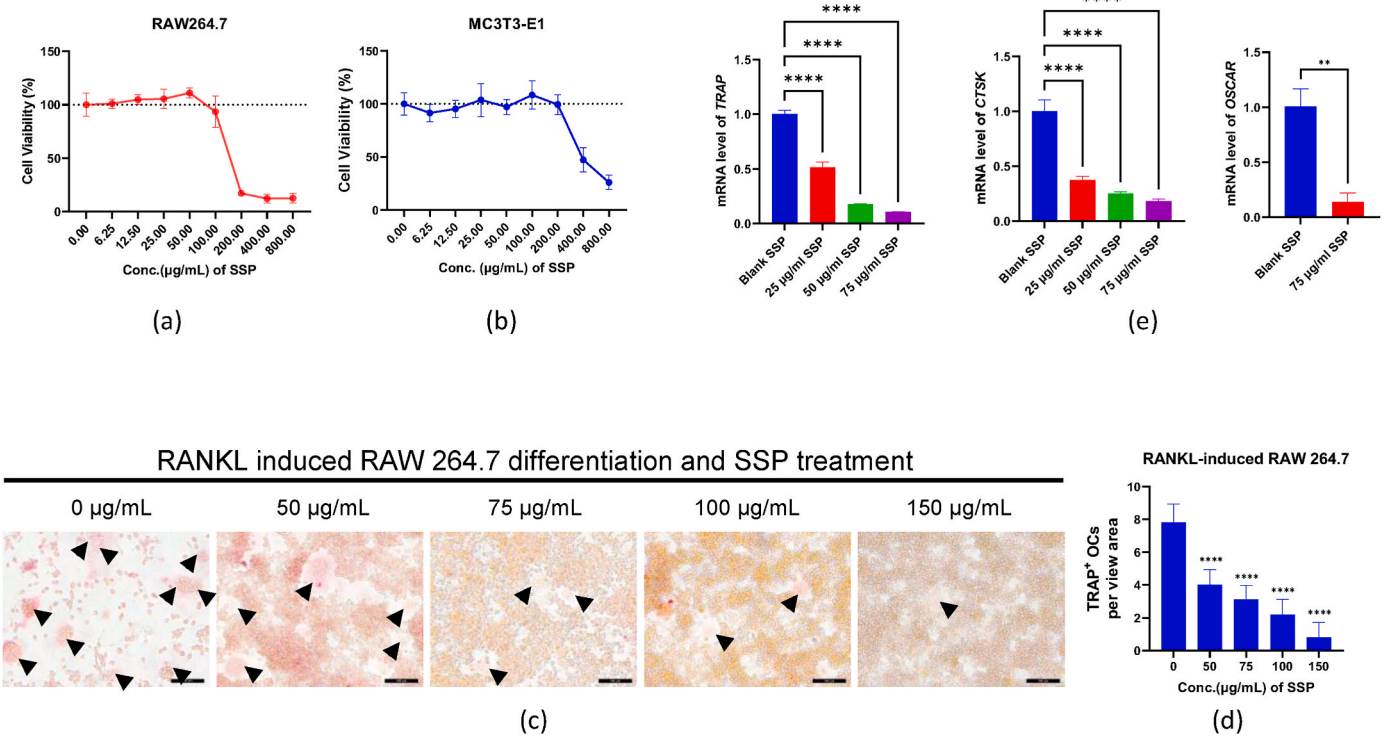

Fig. 2. SSP restrains RANKL-induced osteoclastic differentiation of RAW 264.7 cells *in vitro*. The MTT assay was used to determine the viability of RAW 264.7 cells (a) and MC3T3-E1 cells (b) after SSP treatment (ranging from 0 to 800 g/mL). (c–d) After RANKL (10 ng/mL) induction and SSP treatment (50, 75, 100, 150 μg/mL), TRAP staining of RAW 264.7 cell-derived osteoclasts was conducted. The representative result is shown here, and quantitative analyses of TRAP + mature osteoclasts (black arrow indicates) were performed in pictures of 5–10 random fields under 20 × objective magnification. (e) After RANKL (10 ng/mL) induction and SSP treatment (25, 50, 75 μg/mL), the mRNA expression of osteoclast marker genes (Trap, Ctsk, Oscar) was detected by qPCR assay. The experiments were performed with at least three replicates, and values are presented as the mean ± SD. Data were analyzed in GraphPad Prism 9.0. *P < 0.05, **P < 0.01, and ***P < 0.001 as compared to the control.

3.3. SSP suppresses MDA-MB-231-conditioned medium-induced osteoclastic differentiation in RAW 264.7 cells

As metastatic cancer cells grow and interact with stromal cells in the bone microenvironment, they can secrete various cytokines to stimulate osteoclasts directly or indirectly, resulting tumor-induced osteolysis.[36] A MDA-MB-231 cell-derived conditioned medium (CM) co-culture model was used to determine whether SSP could attenuate the tumor-induced osteolytic bone microenvironment. First, we optimized the ratio of MDA-MB-231-CM by comparing the proliferation and differentiation of RAW264.7 cells. As a result of the data, it was determined that 12.5 %, 25 %, and 50 % CM could promote the growth of RAW264.7 cells (Fig. 3a), while compared with blank group with RANKL only. The number of TRAP-positive cells was increased in 25 %, and 50 % CM intervention groups (Fig. 3b and c). Collectively, the concentration of 25 % CM presented better promotion effects and was used for further experiments.

SSP pre-treatment was applied to the MDA-MB-231-CM-induced osteoclast differentiation model. To eliminate the direct killing effect of SSP on BC cells, the dosage of SSP in this step was kept lower than 40 μg/mL. Then, supernatant medium was obtained from MDA-MB-231 cells that had been pretreated with or without SSP for 24 h, and the following steps were the same as previously described. TRAP staining results revealed that pre-treatment of BC cells with SSP could inhibit tumor cells' induction of the process of pre-osteoclasts differentiating into mature osteoclasts (Fig. 3d and e), The results indicate that some cytokines secreted by MDA-MB-231 cells were reduced by SSP treatment, thereby, slowing or partially blocked differentiation. Dickkopf-related protein 1 (DKK1) is secreted from cancer cells and has a facilitating effect on organotropic bone metastasis.[37] DKK1 expression is positively related to mammary tumor bone metastasis. which can be regarded as a serological biomarker.[37,38] From Fig. 3f, the mRNA expression of gene *Dkk1* was decreased after treatment with SSP, which proves that the tumor microenvironment was improved after SSP treatment. Similarly, the mRNA expression of osteoclast-specific marker genes (*Trap, Ctsk,* and *Oscar*) and the protein expression of CTSK were

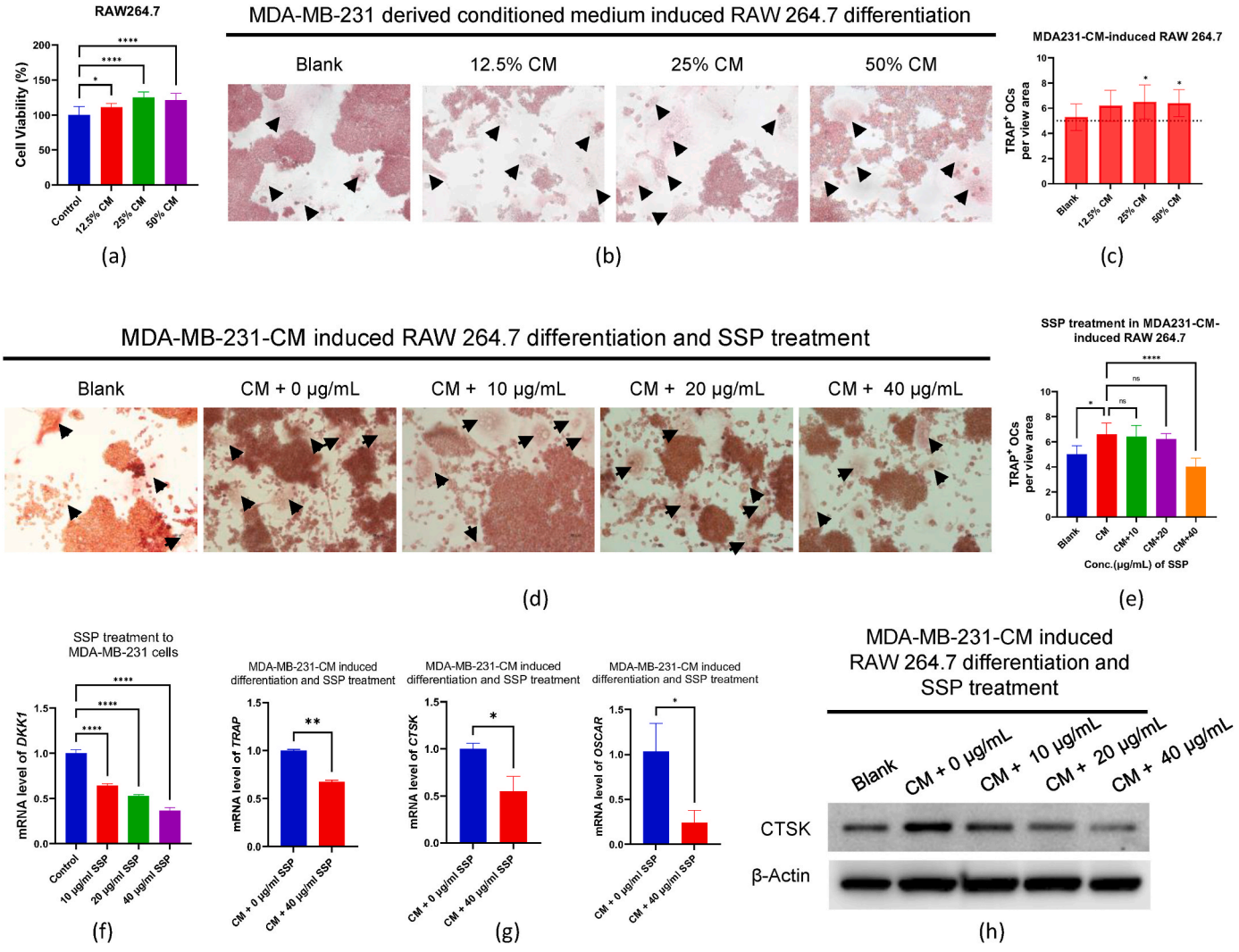

Fig. 3. SSP suppresses MDA-MB-231 cell conditioned medium-induced osteoclastic differentiation of RAW 264.7 cells. (a) The MTT assay was used to detect the viability of RAW 264.7 after different percentages of CM intervention. (b–c) After RANKL and CM induction, TRAP staining of RAW 264.7 cell-derived osteoclasts was conducted. (d–e) After RANKL and SSP-pretreated-CM induction, TRAP staining of RAW 264.7 cell-derived osteoclasts was conducted. The representative result is shown here, and quantitative analyses of TRAP + mature osteoclasts (black arrow indicates) were performed in pictures of 5–10 random fields under 20 × objective magnification. (f) The expression level of Dkk1 in MDA-MB-231 cells after direct SSP treatment was tested by qPCR assay. After inducing SSP-treated (10, 20, 40 μg/mL) MDA-MB-231 CM in RAW264.7 cells, the mRNA expression of osteoclast marker genes (Trap, Ctsk, Oscar) was detected by qPCR assay (g), and the protein expression level of CTSK was tested by Western blotting. The experiments were performed at least three times, and values are presented as the mean ± standard deviation (SD). Data were analyzed in GraphPad Prism 9.0. $^{*}P < 0.05$, $^{**}P < 0.01$, and $^{***}P < 0.001$ as compared to the control/model group.

also conspicuously repressed by SSP treatment in comparison with the CM model group (Fig. 3g and h).

3.4. SSP inhibits breast cancer-bone metastasis in vivo and extends overall survival time

To examine the therapeutic effect of SSP on BC-induced osteolytic bone metastasis, an *in vivo* xenograft bone metastasis model was established by injecting human cancer cells MDA-MB-231 into the left cardiac ventricle as described in Fig. 4a. As shown in Fig. 4b, the median survival time of SSP treatment group (38 days) was significantly longer than that of vehicle control group (33 days). After cell injection for more than 30 days, typical symptoms of bone metastasis such as paralysis, body weight loss, and inactive behaviors were observed. Combined with the results shown in Fig. 4c, bio-fluorescence signals also appeared on the mice' bones, indicating that the model of bone metastasis was successful and that the SSP administration group showed slightly reduced tumor cell luminescence signals (Fig. 4d). According to micro-CT images in Fig. 4e, the SSP administration group had fewer osteolytic bone lesions (Fig. 4f) whereas control group had a much heavier metastatic burden. Therefore, these findings demonstrated that SSP could inhibit BC-induced osteolytic bone metastasis *in vivo* and extend the overall survival time of mice. There is still a need for more effort to apply SSP or drug combination in clinical settings.

4. Discussion

The anti-cancer activity of SS has attracted more attention in recent years. It was reported that SS could arrest the cell cycle,[11] induce BC cell apoptosis through the mitochondrial pathway,[11] caspase-dependent pathway,[16] and promote TNBC cell death through the non-canonical pyroptotic pathway.[12] Interestingly, SS could act as a platelet aggregation inhibitor, allowing SSP to reduce tumor cell survival in the circulation system. This is important in the metastasis process of colorectal cancer,[14] melanoma,[39] and BC.[13] This shares some similarities with the Chinese medicine theory that SS is able to improve blood stasis.[11] It has also been shown that SS is beneficial for treating rheumatic arthralgia in clinics,[10] which indicates it might also be beneficial in treating bone-related diseases, and some papers have already been published.[24–26] However, the protective efficacy and mechanism of SSP against tumor-induced metastasis to bone, the most targeted organ in BC, have not been completely unraveled. In this study, we demonstrated and confirmed the inhibitory effect of SSP not only in the *in vitro* osteoclast differentiation models but also in an *in vivo* BCBM model for the first time. *In vivo* results demonstrated that SSP group significantly prolonged the survival time of mice compared with the vehicle control group. The results were consistent with previous reports,[24,25] that SSP could inhibit the differentiation of osteoclast precursor cells induced by RANKL in a dose-dependent manner, although there was slight difference in that we used RAW264.7 cell as osteoclast precursor cell here, instead of using primary bone marrow-derived macrophage cells isolated from mice. A similar decrease was seen in the mRNA synthesis level of representative markers such as TRAP, CTSK, OSCAR. According to these results, SSP's mechanisms work partly by directly affecting osteoclast precursor cells.

The harmful bone microenvironment plays a critical role in the process of BCBM, initiated by cancer cells, which aggravates the "vicious

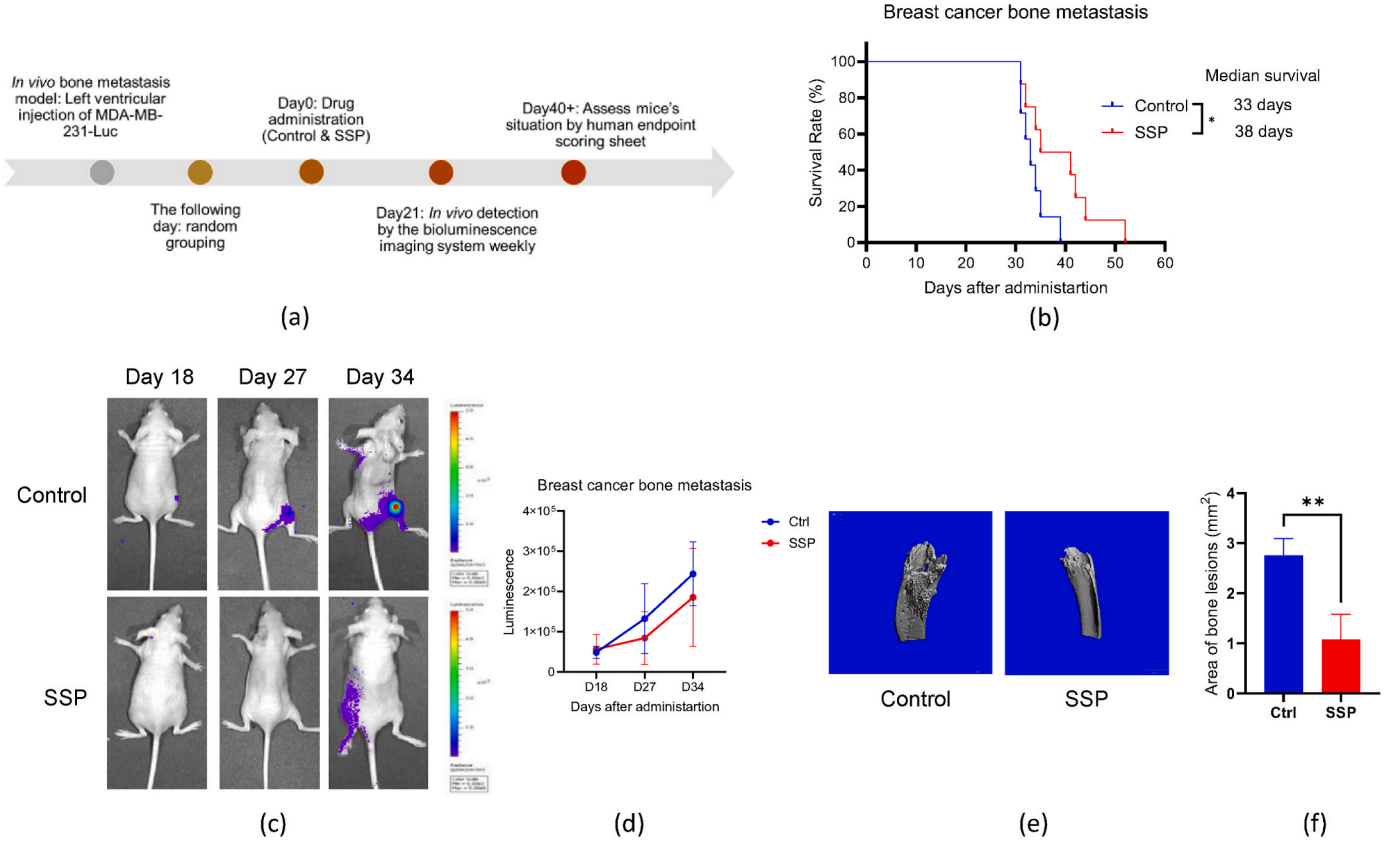

Fig. 4. SSP slows down the breast cancer-bone metastasis process and extends overall mouse survival time *in vivo*. (a) The time axis of the in-vivo treatment schedule. The breast cancer bone metastasis model in nude mice was established by left ventricular injection of MDA-MB-231 transfected with a luciferase plasmid. (b) The overall survival rate in each group (n = 8) was collected during the whole process. A human endpoint sheet was used to assess the mice's situation. A representative bioluminescence image obtained from a small animal imaging system was used to determine the degree of metastasis. (d) The luminescence signals were presented. (e) Representative micro-CT images in each group showed osteolytic bone lesions at the tibia. (f) Area of osteolytic bone lesions in control and SSP group were shown. ~~Survival analysis~~ Statistic data were analyzed in GraphPad Prism 9.0. $^{*}P < 0.05$ and $^{**}P < 0.01$ as compared with the control group.

cycle", resulting in the occurrence of bone resorption, and even fractures. A conditional medium derived from BC was widely used to simulate the pathological environment of cancer cells.[38,40] However, there haven't been any reports to evaluate the efficacy of SSP using this model. Our results here also verify that SSP presents anti-osteoclastogenic efficacy induced by CM derived from MDA-MB-231. Herein, our experimental condition to obtain CM was at a dose of ≤40 μg/mL for 24 h. Therefore, the viability of BC cells was little influenced, and thus, SSP played a therapeutic role partially by improving the microenvironment.

Combined with the significant pharmacological effects of SSP on inhibiting cancer cell proliferation and motility, the present study data indicate that SSP could directly inhibit cancer cells. In addition, SSP could ameliorate the cancer cell microenvironment. Moreover, SS is a medicinal herb that is often used clinically with high safety, and our experiments have also shown that SSP, within 100 μg/mL, displayed very low cytotoxicity to normal pre-osteoclast cell line RAW264.7 or pre-osteoblast cell line MC3T3-E1. Also, acute toxicity studies have reported an LD50 value of 10 g/kg body weight for oral treatment of SS.[12] This indicates that SSP has a potential advantage as a clinical agent against osteolytic bone metastasis in BC.

The main ingredients of SS are flavonoids such as isoliquiritigenin (ISL) and procyanidins such as (epi)-catechin, (epi)-gallocatechin gallate, and their polymers. The anti-BC effects of isoliquiritigenin were confirmed by previous work.[41–43] It has been shown that ISL had inhibitory effects on RANKL-induced osteoclastogenesis and reduces RANKL/osteoprotegerin (OPG) ratio in osteoblast cells,[44,45] but *in vivo* evidence is still needed. Besides, the anti-cancer effect was evaluated by using lactate dehydrogenase A expression, which was higher when (epi)-catechin and (epi)-gallocatechin gallate were combined, which largely relied on the existence of epigallocatechin (EGC).[15] It has been demonstrated that procyanidins from grape seeds, black bean skins, and sea buckthorn seeds may target osteoclasts precursors by suppressing activation and upregulating apoptosis in cancer-associated bone metastasis and osteoporosis.[46,47] Therefore, the effective substances of SSP in anti-bone metastasis needs more exploration, and close attention should also to be paid to investigate whether there is a synergistic effect. Based on the above findings we highlight the clinical significance of SSP as a potential treatment option for breast cancer, particularly in targeting bone metastasis and improving patient outcomes. Further research and clinical trials are needed to validate these promising results and explore the therapeutic potential of SSP in clinical settings for breast cancer patients.

5. Conclusions

In summary, the findings of the present study explicate that *Spatholobus suberectus* Dunn ethanol extract (SSP) mitigates *in vitro* osteoclast differentiation and *in vivo* osteolytic bone metastasis induced by mammary tumors through different aspects (Fig. 5): SSP could (1) possess direct tumor cell killing and cell motility inhibiting abilities; (2) repress osteoclast differentiation induced by RANKL, which is rich in the bone resorption microenvironment; and (3) attenuate osteoclast differentiation induced by MDA-MB-231 conditioned medium. However, more efforts are needed to clarify the mechanisms underlying the anti-bone metastasis efficacy of SSP from different aspects, such as BC cell colonization and osteoclasts recruitment, which may provide new drugs for the prevention and treatment of BCBM.

6. Patents

The extraction technology, fractions and anti-bone metastatic pharmacological activities of SSP are patented by authors. Patent Numbers: CN102579425A, CN113925890A.

CRediT author statement

Conceptualization, J.C., Y.J. and J.L.; *in vitro* experiments, N.L., Q.L. and D.L.; *in vivo* model establishment and experiments, Y.J., Q.L., F.Z. and Y.S.; writing—original draft preparation, Q.L. and N.L.; writing—review and editing, K.G., J.C. and J.L.; funding acquisition, J.C. and J.L. All authors have read and agreed to the published version of the manuscript.

Ethics approval and consent to participate

All experiments were approved by the Guidelines for Laboratory Animal Care and Committee on the Use of Live Animals in Teaching and Research (CULATR No: 5161-19).

Consent for publication

The manuscript is approved by all authors for publication.

Funding

This research was funded by the Innovation and Technology Fund,

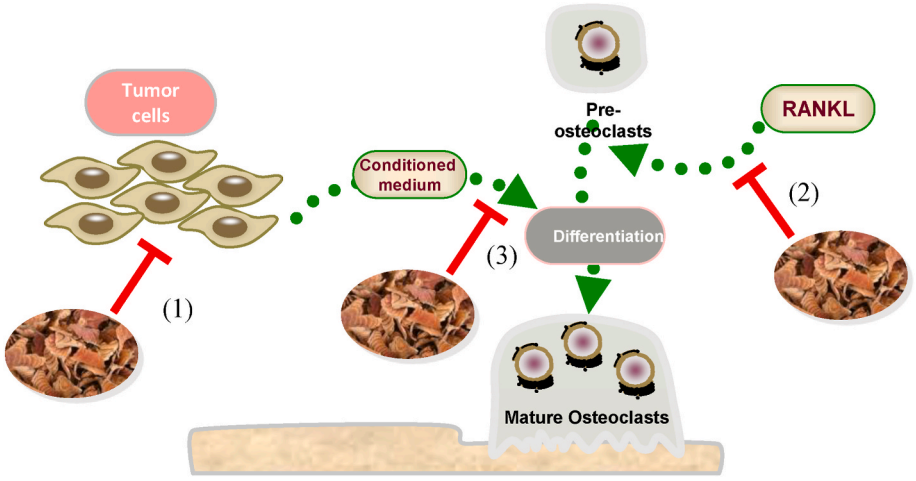

Fig. 5. The overall graphic overview of this study. *Spatholobus suberectus* ethanol extract (termed SSP) displayed anti-breast cancer bone metastasis effects through different aspects: (1) possesses direct tumor cell killing and cell motility inhibiting abilities; (2) represses osteoclast differentiation induced by RANKL, which is rich in the bone resorption microenvironment; and (3) attenuates osteoclast differentiation induced by MDA-MB-231 conditioned medium through lessening DKK1 secretion *in vitro* and tumor-induced osteolytic bone metastasis *in vivo*.

Hong Kong (MRP/027/18X), and Guangxi Science and Technology Key Research and Development Program (AB16450012).

Declaration of competing interest

The authors declare that they have no known competing financial interests or personal relationships that could have appeared to influence the work reported in this paper.

Acknowledgments

The authors acknowledge the assistance of the University of Hong Kong Li Ka Shing Faculty of Medicine Faculty Core Facility, as well as the technical help from Mr. Alex and Mr. Keith and Ms. Cindy in the research laboratory of the School of Chinese Medicine.

References

1. Sung H, Ferlay J, Siegel RL, et al. Global cancer Statistics 2020: GLOBOCAN estimates of incidence and mortality worldwide for 36 cancers in 185 countries. *CA Cancer J Clin*. 2021;71(3):209–249.
2. Coleman RE. Clinical features of metastatic bone disease and risk of skeletal morbidity. *Clin Cancer Res*. 2006;12(20 Pt 2):6243s–6249s.
3. Zhou X, Liu M, Zheng Z, et al. Nomogram predicts survival and surgical benefits for patients with breast cancer with initial bone metastasis: a population-based study. *Cancer*. 2024;130(S8):1464–1475.
4. Shupp AB, Kolb AD, Mukhopadhyay D, Bussard KM. Cancer metastases to bone: concepts, mechanisms, and interactions with bone osteoblasts. *Cancers*. 2018;10(6).
5. Knapp BJ, Cittolin-Santos GF, Flanagan ME, et al. Incidence and risk factors for bone metastases at presentation in solid tumors. *Front Oncol*. 2024;14, 1392667.
6. Steinvoort-Draat IN, Otto-Vollaard L, Quint S, Tims JL, de Pree IMN, Nuyttens JJ. Palliative radiotherapy: new prognostic factors for patients with bone metastasis. *Cancer Radiother*. 2024;28(3):236–241.
7. Coleman RE, Croucher PI, Padhani AR, et al. Bone metastases. *Nat Rev Dis Primers*. 2020;6(1):83.
8. Park JH, Son YJ, Lee CH, Nho CW, Yoo G. Circaea mollis Siebold & Zucc. Alleviates postmenopausal osteoporosis in a mouse model via the BMP-2/4/Runx2 pathway. *BMC Complement Med Ther*. 2020;20(1):123.
9. Wang M, Xia F, Wei Y, Wei X. Molecular mechanisms and clinical management of cancer bone metastasis. *Bone Res*. 2020;8(1):30.
10. Tang P, Liu H, Lin B, et al. Spatholobi Caulis dispensing granule reduces deep vein thrombus burden through antiinflammation via SIRT1 and Nrf2. *Phytomedicine*. 2020;77, 153285.
11. Wang ZY, Wang DM, Loo TY, et al. Spatholobus suberectus inhibits cancer cell growth by inducing apoptosis and arresting cell cycle at G2/M checkpoint. *J Ethnopharmacol*. 2011;133(2):751–758.
12. Zhang F, Liu Q, Ganesan K, et al. The antitriple negative breast cancer efficacy of Spatholobus suberectus Dunn on ROS-induced noncanonical inflammasome pyroptotic pathway. *Oxid Med Cell Longev*. 2021;2021, 5187569.
13. Chen X, Li Q, Kan XX, et al. Extract of Caulis Spatholobi, a novel blocker targeting tumor cell-induced platelet aggregation, inhibits breast cancer metastasis. *Oncol Rep*. 2016;36(6):3215–3224.
14. Sun L, Li Q, Guo Y, et al. Extract of Caulis Spatholobi, a novel platelet inhibitor, efficiently suppresses metastasis of colorectal cancer by targeting tumor cell-induced platelet aggregation. *Biomed Pharmacother*. 2020;123, 109718.
15. Wang Z, Wang D, Han S, et al. Bioactivity-guided identification and cell signaling technology to delineate the lactate dehydrogenase A inhibition effects of Spatholobus suberectus on breast cancer. *PLoS One*. 2013;8(2), e56631.
16. Ha ES, Lee EO, Yoon TJ, et al. Methylene chloride fraction of Spatholobi Caulis induces apoptosis via caspase dependent pathway in U937 cells. *Biol Pharm Bull*. 2004;27(9):1348–1352.
17. Liu B, Liu J, Chen J, Zhu D, Zhou H, Wang X. A study on anticancer activity of Caulis Spatholobi extract on human osteosarcoma Saos-2 cells. *Afr J Tradit Complement Altern Med*. 2013;10(5):256–260.
18. Kim H, Yi SS, Lee HK, et al. Antiproliferative effect of vine stem extract from Spatholobus suberectus Dunn on rat C6 glioma cells through regulation of ROS, mitochondrial depolarization, and P21 protein expression. *Nutr Cancer*. 2018;70(4):605–619.
19. Wang N, Wang J, Meng X, Bao Y, Wang S, Li T. 3D microfluidic in vitro model and bioinformatics integration to study the effects of Spatholobi Caulis tannin in cervical cancer. *Sci Rep*. 2018;8(1), 12285.
20. Lim HJ, Park MN, Kim C, et al. MiR-657/ATF2 signaling pathway has a critical role in Spatholobus suberectus Dunn extract-induced apoptosis in U266 and U937 cells. *Cancers*. 2019;11(2).
21. Zhang F, Ganesan K, Liu Q, Chen J. A review of the pharmacological potential of Spatholobus suberectus Dunn on cancer. *Cells*. 2022;11(18):2885.
22. Xie F, Wang M, Su Y, et al. Unveiling potential mechanisms of spatholobi caulis against lung metastasis of malignant tumor by network pharmacology and molecular docking. *Evid Based Complement Alternat Med*. 2024;2024, 1620539.
23. Zhu SC, Cai J, Wu CY, Cheng CS. [Molecular mechanism of Spatholobi Caulis in treatment of ovarian cancer based on network pharmacology and experimental verification]. *Zhongguo Zhongyao Zazhi*. 2022;47(3):786–795.
24. Ha H, Shim KS, An H, Kim T, Ma JY. Water extract of Spatholobus suberectus inhibits osteoclast differentiation and bone resorption. *BMC Complement Altern Med*. 2013;13:112.
25. Im NK, Lee SG, Lee DS, Park PH, Lee IS, Jeong GS. Spatholobus suberectus inhibits osteoclastogenesis and stimulates chondrogenesis. *Am J Chin Med*. 2014;42(5):1123–1138.
26. Toyama T, Todoki K, Takahashi Y, et al. Inhibitory effects of Jixueteng on P. gingivalis-induced bone loss and osteoclast differentiation. *Arch Oral Biol*. 2012;57(11):1529–1536.
27. Liu J, Li D, Dang L, et al. Osteoclastic miR-214 targets TRAF3 to contribute to osteolytic bone metastasis of breast cancer. *Sci Rep*. 2017;7, 40487.
28. Ribatti D, Tamma R, Annese T. Epithelial-mesenchymal transition in cancer: a historical overview. *Transl Oncol*. 2020;13(6), 100773.
29. Liu X, Riquelme MA, Tian Y, et al. ATP inhibits breast cancer migration and bone metastasis through down-regulation of CXCR4 and purinergic receptor P2Y11. *Cancers*. 2021;13(17).
30. Zhang Z, Yao Y, Yuan Q, et al. Gold clusters prevent breast cancer bone metastasis by suppressing tumor-induced osteoclastogenesis. *Theranostics*. 2020;10(9):4042–4055.
31. Jiang P, Gao W, Ma T, et al. CD137 promotes bone metastasis of breast cancer by enhancing the migration and osteoclast differentiation of monocytes/macrophages. *Theranostics*. 2019;9(10):2950–2966.
32. Shen X, Sun X, Chen H, et al. Demethoxycucumin protects MDA-MB-231 cells induced bone destruction through JNK and ERK pathways inhibition. *Cancer Chemother Pharmacol*. 2021;87(4):487–499.
33. Salvador F, Llorente A, Gomis RR. From latency to overt bone metastasis in breast cancer: potential for treatment and prevention. *J Pathol*. 2019;249(1):6–18.
34. Brook N, Brook E, Dharmarajan A, Dass CR, Chan A. Breast cancer bone metastases: pathogenesis and therapeutic targets. *Int J Biochem Cell Biol*. 2018;96:63–78.
35. Li D, Liu J, Guo B, et al. Osteoclast-derived exosomal miR-214-3p inhibits osteoblastic bone formation. *Nat Commun*. 2016;7, 10872.
36. Maroni P, Bendinelli P. Bone, a secondary growth site of breast and prostate carcinomas: role of osteocytes. *Cancers*. 2020;12(7).
37. Zhuang X, Zhang H, Li X, et al. Differential effects on lung and bone metastasis of breast cancer by Wnt signalling inhibitor DKK1. *Nat Cell Biol*. 2017;19(10):1274–1285.
38. Yue Z, Niu X, Yuan Z, et al. RSPO2 and RANKL signal through LGR4 to regulate osteoclastic premetastatic niche formation and bone metastasis. *J Clin Invest*. 2022;132(2).
39. Kang IC, Kim SA, Song GY, et al. Effects of the ethyl acetate fraction of Spatholobi caulis on tumour cell aggregation and migration. *Phytother Res*. 2003;17(2):163–167.
40. Taipaleenmaki H, Browne G, Akech J, et al. Targeting of runx2 by miR-135 and miR-203 impairs progression of breast cancer and metastatic bone disease. *Cancer Res*. 2015;75(7):1433–1444.
41. Wang N, Wang Z, Peng C, et al. Dietary compound isoliquiritigenin targets GRP78 to chemosensitize breast cancer stem cells via beta-catenin/ABCG2 signaling. *Carcinogenesis*. 2014;35(11):2544–2554.
42. Peng F, Tang H, Liu P, et al. Isoliquiritigenin modulates miR-374a/PTEN/Akt axis to suppress breast cancer tumorigenesis and metastasis. *Sci Rep*. 2017;7(1):9022.
43. Peng F, Du Q, Peng C, et al. A review: the pharmacology of isoliquiritigenin. *Phytother Res*. 2015;29(7):969–977.
44. Lee SK, Park KK, Park JH, Lim SS, Chung WY. The inhibitory effect of roasted licorice extract on human metastatic breast cancer cell-induced bone destruction. *Phytother Res*. 2013;27(12):1776–1783.
45. Lee SK, Park KK, Kim KR, Kim HJ, Chung WY. Isoliquiritigenin inhibits metastatic breast cancer cell-induced receptor activator of nuclear factor kappa-B ligand/osteoprotegerin ratio in human osteoblastic cells. *J Cancer Prev*. 2015;20(4):281–286.
46. Guo S, Zhu W, Yin Z, et al. Proanthocyanidins attenuate breast cancer-induced bone metastasis by inhibiting Irf-3/c-jun activation. *Anti Cancer Drugs*. 2019;30(10):998–1005.
47. Zhu W, Yin Z, Zhang Q, et al. Proanthocyanidins inhibit osteoclast formation and function by inhibiting the NF-kappaB and JNK signaling pathways during osteoporosis treatment. *Biochem Biophys Res Commun*. 2019;509(1):294–300.